Journal of Undergraduate Chemistry Research, **2026**, 25 (4), 138

RUTHENIUM-CATALYZED OXIDATIVE DEHYDROGENATION OF INDOLINES UNDER AEROBIC CONDITIONS

Holden Petty*, Wyatt Evans*, Morgan Whitaker*, Tesla Shafer* and Matthew B. Prater†

Department of Chemistry and Physics, Southern Utah University, Cedar City, UT 84720

Abstract

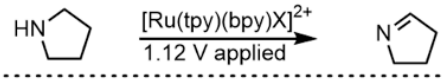
This report details the Ru(III)-catalyzed oxidative dehydrogenation of indoline derivatives to indoles under aerobic conditions, affording isolated yields of up to 94%. Optimization studies identified tetrahydrofuran and molecular oxygen addition as key parameters for efficient catalysis. Substrate scope investigations revealed that electron-rich indoline derivatives undergo oxidation more readily than electron-deficient substrates. Additionally, exploratory mechanistic studies employing phosphine ligands and cyclic voltammetry were conducted to probe the possible formation of low-valent ruthenium intermediates. While phosphine additives significantly altered catalytic activity, cyclic voltammetry experiments did not support the presence of a persistent, electrochemically observable Ru(I) intermediate under the conditions examined. These findings provide insight into the behavior of in situ generated Ru-based oxidation catalysts for indole synthesis.

†Corresponding author: matthewprater@suu.edu *Undergraduate researchers and co-authors
Keywords: catalysis, oxidative dehydrogenation, cyclic voltammetry, square wave voltammetry, indole
Received: September 30, 2026 Accepted: October 26, 2026 Revision received: November 3, 2026 Published: November 10, 2026

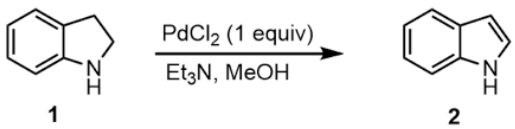
Introduction

Indole and its derivatives have attracted considerable attention due to their widespread presence in biologically active compounds, natural products, and pharmaceutical agents[1,2]. Traditional methods for the synthesis of indoles include the Fischer,[3] Leimgruber–Batcho,[4] Bartoli,[5] and Larock indole syntheses.[6] More recent developments have focused on transition-metal-catalyzed methodologies,[7] including intramolecular C–H amination reactions and dehydrogenative cyclization of vinyl anilines.[8] In addition to direct indole-forming reactions, oxidative dehydrogenation of indolines represents an attractive strategy for indole synthesis due to the accessibility of indoline precursors and the simplicity of the transformation. Keene and coworkers reported Ru-assisted oxidation of amines to imines under oxidative conditions (Scheme 1a),[9,10] while Kuehne and coworkers demonstrated that transition metals such as Pd(II) and Au(III) can mediate the oxidation of indoline to indole (Scheme 1b).[11] As ruthenium has previously been used to oxidize amines,[12,13] we sought to investigate the use of an *in situ* generated Ru-catalyst system for the oxidation of indoline derivatives to indoles (Scheme 1c).

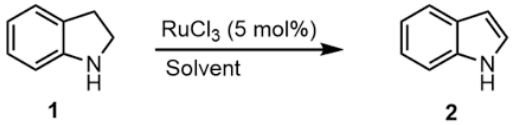
Scheme 1a. Oxidation of Secondary Amines



Scheme 1b. Pd-Mediated Oxidation of Indoline



Scheme 1c. Proposed Work



Scheme 1. A. Previous work involving oxidation of secondary amines with Ru. **B**. Previous oxidation of indoline with stoichiometric Pd. **C**. Proposed oxidation of indoline.

Experimental

General Considerations

Indoline was freshly distilled, while 5-methoxyindoline and 5-methylindoline were purchased as the hydrochloride salts and were deprotonated with saturated aqueous sodium bicarbonate solution and washed with ethyl acetate before being dried under vacuum before use. The ethyl acetate was removed under vacuum prior to use in the reaction. All other reagents were used without further purification. Analytical instruments utilized for this work included a Bruker 400 MHz NMR and an Agilent GC/MS. Reagents were generally purchased through Fisher Scientific, but substituted indoline derivatives were purchased through Combi-Blocks.

General Procedure for Catalytic Oxidation

In a 20 mL scintillation vial equipped with a rubber septum was added the indoline substrate (0.5 mmol), ruthenium(III) chloride (0.025 mmol, 5 mol%), and THF (5 mL). Oxygen gas was bubbled through the solvent for 5 minutes, and the reaction was stirred for 24 hours under an oxygen atmosphere using an oxygen-filled balloon. Following completion, the solvent was removed under vacuum, and the crude mixture was purified by silica gel column chromatography using ethyl acetate/hexanes. Purified products were analyzed by ^{1}H NMR spectroscopy, and spectroscopic data were compared to literature values.

Substrate Scope

indole

The general procedure was followed with indoline (60. mg, 0.5 mmol), $RuCl_3$ (5.6 mg, 0.025 mmol), and THF (5 mL). Following solvent removal under vacuum, the crude mixture was purified via silica gel column chromatography (hexanes:ethyl acetate 90:10) to yield a pale purple solid (47 mg, 81% yield). R_f = 0.25 (10% ethyl acetate/hexanes). Spectroscopic data matched the literature[2].[17]

2-methylindole

The general procedure was followed with modifications

involving 2-methylindoline (670 mg, 5.0 mmol), $RuCl_3$ (5.6 mg, 0.025 mmol, 0.50 mol%), and THF (5 mL). Following solvent removal under vacuum, the crude mixture was purified via silica gel chromatography (gradient elution, hexanes to hexanes:ethyl acetate 90:10) to yield a pale yellow solid (600 mg, 92% yield). R_f = 0.25 (hexanes:ethyl acetate 75:25). Spectroscopic data matched the literature.[15]

5-bromoindole

The general procedure was followed with modifications involving 5-bromoindoline (990 mg, 5.0 mmol), $RuCl_3$ (5.6 mg, 0.025 mmol, 0.50 mol%), and THF (5 mL). Following solvent removal under vacuum, the crude mixture was purified via silica gel chromatography (gradient elution, hexanes to hexanes:ethyl acetate 90:10) to yield a pale yellow solid (890 mg, 91% yield). Rf = 0.5 (hexanes:ethyl acetate 80:20). Spectroscopic data matched the literature.[17]

5-methoxyindole

The general procedure was followed with modifications involving 5-methoxyindoline (150 mg, 1.0 mmol), $RuCl_3$ (10. mg, 5 mol%), and THF (5 mL). Following solvent removal under vacuum, the crude mixture was purified via silica plug (hexanes:ethyl acetate 1:1) to yield a dark blue/green solid (130 mg, 88% yield). R_f = 0.29 (hexanes:ethyl acetate 90:10). Spectroscopic data matched the literature.[17]

5-methylindole

The general procedure was followed with scale modifications involving 5-methylindoline (130 mg, 1.0 mmol), $RuCl_3$ (10. mg, 0.05 mmol 5 mol%), and THF (5 mL). Following solvent removal under vacuum, the crude mixture was purified via silica gel chromatography (gradient elution, hexanes to hexanes:ethyl acetate 90:10) to yield a pale brown solid (120 mg, 94% yield). Rf = 0.27 (hexanes:ethyl acetate 90:10). Spectroscopic data matched the literature.[17]

5-nitroindole

The general procedure was followed with scale modifications 5-nitroindoline (410 mg, 2.5 mmol), $RuCl_3$ (26 mg, 0.13 mmol), and THF (5 mL). Following solvent removal under vacuum, the crude mixture was purified via silica gel column chromatography (gradient elution, hexanes to hexanes:ethyl acetate 80:20) to yield a yellow solid (290 mg, 72% yield). Rf = 0.18 (20% ethyl acetate/hexanes). Spectroscopic data matched the literature.[17]

5-bromo-7-nitro-1H-indole

The general procedure was followed with scale modifications involving 5-bromo-7-nitroindoline (24 mg, 0.10 mmol), $RuCl_3$ (2.2 mg, 10 mol%), and THF (1 mL). Following solvent removal under vacuum, the crude mixture was purified via silica plug (ethyl acetate) and analyzed via GC/MS. Conversion was 15% and no further purification was conducted.

methyl 1H-indole-5-carboxylate

The general procedure was followed with methyl indoline-5-carboxylate (890 mg, 5.0 mmol), $RuCl_3$ (100 mg, 0.50 mmol, 10 mol%), and THF (5 mL). Following solvent removal under vacuum, the crude mixture was purified via silica gel column chromatography (gradient elution, hexanes to hexanes:ethyl acetate 80:20) to yield a pale yellow solid (590 mg, 67% yield). Rf = 0.23 (20% ethyl acetate/hexanes). Spectroscopic data matched the literature.[19]

methyl indole-2-carboxylate

The general procedure was followed with methyl (2*S*)-2,3-dihydroindoline-2-carboxylate (180 mg, 1.0 mmol), $RuCl_3$ (10. mg, 5 mol%), and THF (5 mL). Following solvent removal under vacuum, the crude mixture was purified via silica plug (ethyl acetate) and analyzed via GC/MS. Conversion was 16% and no further purification was conducted.

Phosphine Trials

Reactions were prepared following the general reaction shown in scheme 1. All reactions were prepared using 1 dram glass vials and 1 cm Teflon stir bars, with 0.1 mmol indoline, 0.03 mmol trial specific phosphine, and 0.01 mmol ruthenium(III) chloride dissolved in 1 ml of acetonitrile. For trials 10-12 (Table 3), THF was used in place of acetonitrile under an oxygen atmosphere; all other reaction parameters were maintained as described above. Reaction vessels were flushed with argon and sealed with a rubber septum, which was then fitted with argon-filled balloons to maintain a positive pressure. Vessels were then wrapped in aluminum foil and set to stir for 48 hours, at which point stirring was stopped. A liquid-liquid extraction was performed using approximately 10 mL of deionized water and 10 mL of ethyl acetate. The organic layer was separated and passed through a silica plug with an additional 10 ml of ethyl acetate after loading to remove any remaining water/water soluble impurities. 0.1 – 0.5 ml portions of the organic layer were then diluted in dichloromethane and analyzed via GC-MS. Percent conversions were then calculated using peak area comparison of indole/indoline. For each phosphine tested, reactions were run in duplicate. Organics from each trial were then run triplicate on GC-MS.

Cyclic Voltammetry

Cyclic voltammetry (CV) experiments were carried out using a 10 mL 3-neck round bottom flask. Experiments were conducted using a standard three electrode system of glassy carbon (working), platinum (auxiliary), and silver (pseudo-reference) electrodes. Potentials are reported versus the Ag-wire pseudo-reference electrode and were not referenced to an internal standard. The flask was fitted with rubber septa to seal the vessel around the electrodes. The vessel was then flushed with argon, and reactants were added as stock solutions through the septum via syringe. All electrochemical measurements were carried out in acetonitrile containing 0.10 M tetrabutylammonium bromide (TBAB) as the supporting electrolyte, using stock solutions of anhydrous ruthenium(III) chloride (7.5 mM), triphenylphosphine (22.5 mM), and indoline (500 mM). The anhydrous $RuCl_3$ was sonicated in acetonitrile to promote dissolution; however, small amounts of undissolved material may have remained. Solutions of indoline and triphenylphosphine were prepared fresh to avoid oxidative degradation. Blank trials of each reagent in electrolyte were conducted, followed by general reaction mixtures (Figure 1) with varying molar ratios. The scan rate for all CV data shown is 50 mV/s.

Square Wave Voltammetry

Square-wave voltammetry (SWV) was carried out following CV data collection using the same solutions. Measurements were

performed using an initial potential of +0.800 V and a final potential of −1.500 V, with a potential increment of 0.004 V, pulse amplitude of 0.025 V, frequency of 15 Hz, and a quiet time of 2 s.

Results and Discussion

We initially selected tetrahydrofuran (THF) as the reaction solvent due to the solubility of the ruthenium precursor and associated reagents in this medium. Under initial conditions using 10 mol% Ru, the reaction proceeded to 37% conversion of indoline to indole as determined by GC-MS analysis. The addition of benzoquinone as an external oxidant resulted in decreased conversion, suggesting that strongly oxidizing conditions are detrimental to catalytic performance. Performing the reaction in the absence of light did not lead to any observable improvement in conversion, indicating that photochemical activation is not a contributing factor under these conditions.

Atmospheric effects were then evaluated, and exposure to ambient air resulted in reduced reaction efficiency relative to controlled conditions, suggesting that oxygen or water exposure may negatively impact catalyst formation or stability. Solvent screening revealed that switching from THF to acetonitrile significantly diminished product formation. However, when molecular oxygen was introduced as an oxidant in acetonitrile, conversion improved relative to the non-oxidative conditions, indicating a beneficial role of oxygen in the reaction.

Based on these observations, THF was retained as the optimal solvent and molecular oxygen was introduced in a controlled manner as a terminal oxidant under a controlled oxygen atmosphere. Under these conditions, a marked improvement in conversion was observed. Additionally, reducing the catalyst loading led to further enhancement of efficiency, with optimized conditions affording up to 99% conversion of indoline to indole.

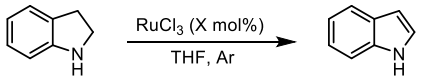
Additionally, control reactions were conducted by not including Ru in a reaction. ~15% conversion was observed, indicating a slow background reaction converting indoline to indole in the presence of oxygen. Although a background reaction was observed in the absence of Ru, the substantially higher conversion obtained in the presence of Ru indicates that ruthenium significantly accelerates the oxidation. The addition of a radical inhibitor, TEMPO, had little effect on the outcome of the reaction, and adding a phosphine with THF as the solvent did not affect the % conversion.

With optimized conditions established, the substrate scope of the catalytic oxidation was evaluated using a series of substituted indoline derivatives. Optimization experiments were evaluated by GC-MS and are reported as percent conversion, whereas substrate-scope reactions were isolated and are reported as isolated yields unless otherwise noted. A clear substituent-dependent trend was observed. Electron-withdrawing groups generally decreased reaction efficiency, with 5-nitro- and methyl ester–substituted substrates affording 72% and 67% yields, respectively. The presence of multiple electron-withdrawing substituents resulted in a near-complete suppression of reactivity to generate the product in only 15% conversion and an ester group at the 2-position was similar with 16% conversion, indicating a strong deactivation effect on the transformation.

In contrast, a mildly deactivating halogen substituent at the 5-position improved the reaction outcome, with 5-bromoindoline providing a 91% yield, even with 0.5 mol% [Ru]. The high yield observed for 5-bromoindole suggests that the observed substituent effect is not governed solely by electronic donation, and additional steric or coordination effects may contribute. Electron-donating substituents were found to further enhance reactivity; 2-methylindoline afforded a 92% yield (also with 0.5 mol% [Ru], while the corresponding 5-methyl derivative gave 94% yield. 5-methoxyindoline was formed in 88% yield.

Overall, these results indicate that electron-rich indoline substrates generally exhibited higher reactivity under the optimized catalytic conditions, possibly due to increased coordination with the Ru(III) or increased stabilization of a cationic or radical intermediate. In contrast, strongly electron-deficient systems diminish reactivity.

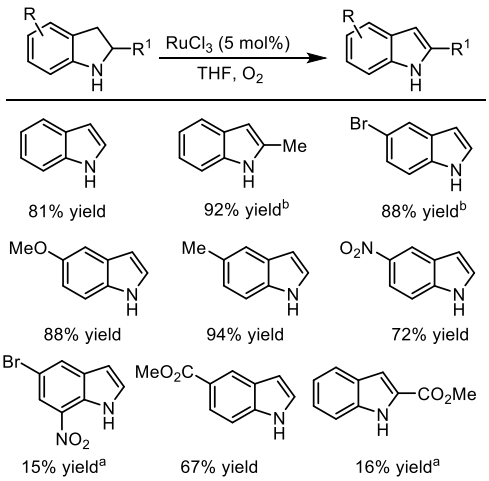
Table 1. Reaction Optimization



Experiment	Change	mol%	% Conversion[a]
1	N/A	10	37
2	Benzoquinone	10	6
3	Dark, BQ	10	5
4	Air	10	10
5	MeCN	10	<5
6	MeCN, O_2	10	38
7	O_2	10	67
8	O_2	5	>99
9	O_2	0	15
10	TEMPO	5	>99
11	O_2, TEMPO	0	<5
12	PPh_3 (15 mol%)	5	>99

[a]Assigned using peak areas on GC/MS.

Table 2. Reaction Scope

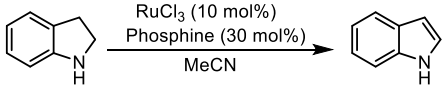


Isolated yields. [a]% conversion using peak ratios on GC/MS
[b]0.5 mol% [Ru] used

Furthermore, we anticipated the formation of a Ru(I) intermediate during the catalytic cycle, as oxidation of indoline to indole formally requires the loss of two electrons. To further probe this possibility, phosphine ligands were investigated during reaction optimization in an effort to stabilize low-valent ruthenium intermediates and better understand the catalytic mechanism. Because acetonitrile provided improved solubility and compatibility for electrochemical studies, phosphine and cyclic voltammetry experiments were conducted in this solvent despite THF providing superior catalytic performance under the optimized synthetic conditions. Accordingly, these electrochemical experiments were used to examine the accessible redox behavior of the Ru/indoline/PPh_3 system rather than to directly reproduce the catalytic reaction conditions.

In acetonitrile, the addition of phosphine ligands resulted in significantly reduced conversion rates, with all phosphine-containing reactions affording less than 20% conversion. This diminished reactivity suggests that strong phosphine coordination may inhibit substrate binding or suppress the formation of catalytically active ruthenium species under these conditions. However, the effect of phosphine addition was strongly dependent on the reaction solvent. When selected phosphine-containing reactions were repeated in THF, conversion increased substantially, with triphenylphosphine, tris(perfluorophenyl)phosphine, and tris(o-tolyl)phosphine each affording greater than 99% conversion (Table 3). This contrast suggests that solvent coordination and the resulting ruthenium speciation play important roles in determining catalytic activity. Within the acetonitrile series, phosphines bearing electron-withdrawing substituents generally provided higher conversions than electron-rich analogues. Additionally, tris(tolyl)phosphine isomers exhibited different reactivities depending on substitution pattern (Table 3), highlighting the sensitivity of the catalytic system to relatively small steric changes surrounding the metal center. Collectively, these observations suggest that both the electronic and steric environment around ruthenium, as well as the reaction solvent, influence catalytic activity. Changes in coordination geometry may contribute to these effects.

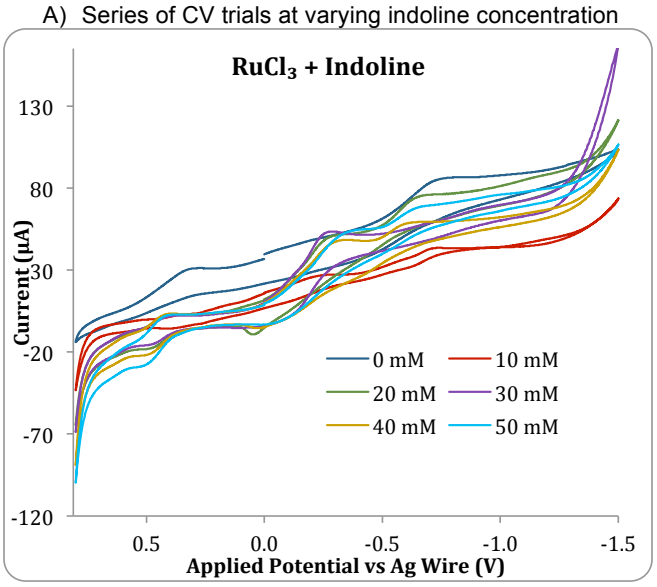
Table 3. Addition of phosphines



Trial	Phosphine	% Conversion[a]
1	Tris(4-fluorophenyl)	18
2	Tris(2-cyanoethyl)	18
3	Tris(perfluorophenyl)	19
4	Tris(*m*-tolyl)	19
5	Tris(*o*-tolyl)	16
6	Tris(*p*-tolyl)	12
7	Tris(2-furyl)	12
8	Bis(diphenylphosphino)methane	12
9	Triphenyl	10
10	Triphenyl[b]	>99
11	Tris(perfluorophenyl)[b]	>99
12	Tris(*o*-tolyl)[b]	>99

[a]Assigned using peak areas on GC/MS. [b]THF used as solvent.

Electrochemical investigations were subsequently carried out using cyclic voltammetry (CV) to probe the possible formation of low-valent ruthenium intermediates. Most notably, none of the reaction mixtures examined exhibited a well-defined reversible redox couple that could be assigned to a persistent Ru(I)/Ru(II) couple (Figure 1). Instead, the voltammograms were characterized by predominantly irreversible electrochemical features, with no clearly resolved corresponding return peaks, and pronounced changes in wave shape upon addition of indoline and PPh_3. The interpretation of these features and their concentration-dependent behavior follows established approaches for evaluating irreversible and chemically coupled electrochemical processes.[14-16] For $RuCl_3$ alone, a prominent cathodic feature was observed near +0.1 V vs Ag wire, whereas addition of indoline substantially altered the voltammogram and produced a large increase in current at more negative potentials. Instead, the voltammograms were character-



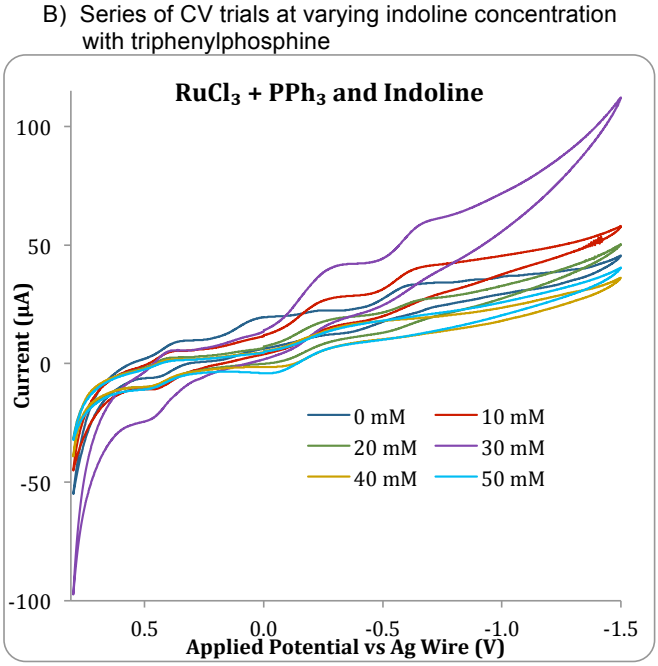
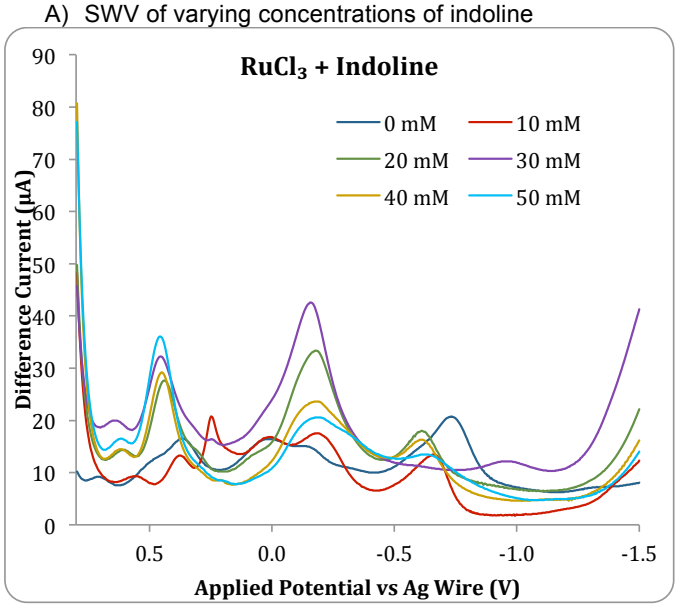


Figure 1. Cyclic voltammetry of varied indoline concentrations in acetonitrile with 5 mM $RuCl_3$ and 0.1 M TBAB. Scan rates are 50 mV/s. A) No phosphine was added. B) Triphenylphosphine was added (10 mM).

ized by predominantly irreversible electrochemical features, with no clearly resolved corresponding return peaks, and pronounced changes in wave shape upon addition of indoline and PPh_3. The interpretation of these features and their concentration-dependent behavior follows established approaches for evaluating irreversible and chemically coupled electrochemical processes.[14-16] In both cases, the 30 mM concentration of indoline exhibited unusually high currents. This concentration was conducted in duplicate with nearly identical results. An additional broad feature was observed in the region of +0.4 to +0.5 V during the final negative-direction portion of the scan, with its current response varying substantially with reaction composition. Addition of PPh_3 attenuated this indoline-dependent current response and produced a substantially different voltammetric profile. The concentration-dependent cathodic shift observed near −0.25 V in the absence of PPh_3 may indicate that the electrochemical response is influenced by a subsequent chemical reaction involving an electrochemically generated ruthenium species. Such behavior could be consistent with an electrochemical-chemical (EC) process, in which electron transfer is followed by a chemical reaction of the generated species. The comparatively smaller potential shift observed in the presence of PPh_3 suggests that the phosphine ligand may influence this subsequent reactivity, potentially through changes in ruthenium coordination or speciation. However, the observed potential shift alone does not establish an EC mechanism. These observations do not support our initial hypothesis of a persistent Ru(I) intermediate participating directly in a simple reversible catalytic cycle. Low-valent ruthenium species could instead be generated only transiently and rapidly undergo secondary reactivity, ligand exchange, or disproportionation before they can be observed on the reverse scan. Alternatively, Ru(I) species observed under sufficiently reducing conditions may be generated electrochemically at the electrode surface rather than representing an appreciably populated catalytic intermediate. Overall, the differences between the phosphine-containing and phosphine-free voltammograms suggest that the ligand environment and competition for coordination in acetonitrile substantially influence the electrochemical behavior of the ruthenium species. These results are consistent with a more complex redox process involving potentially coupled chemical reactions rather than a simple, reversible Ru(I)/Ru(II) redox cycle.

A) SWV of varying concentrations of indoline



B) SWV of varying concentrations of indoline with added phosphine

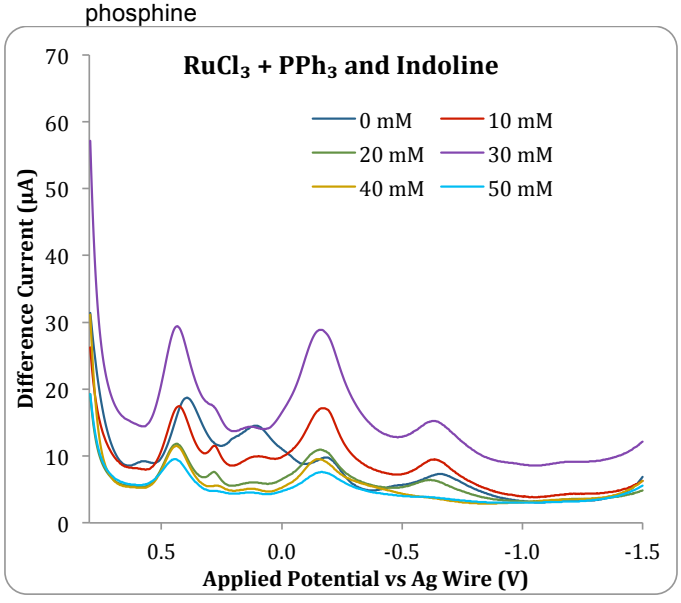


Figure 2. Square wave voltammetry. Each sample was 5 mM $RuCl_3$ in acetonitrile with 0.1 M TBAB. The concentration of indoline was varied. SWV data are reported as the instrument-derived difference current between the forward and reverse components. SWV parameters: 4 mV increment, 25 mV amplitude, and 15 Hz frequency. A) No Phosphine. B) 10 mM PPh_3.

Square-wave voltammetry (SWV) provided additional evidence that both indoline and PPh_3 alter the electrochemical speciation of ruthenium (Figure 2). Because SWV provides complementary information about electrochemical responses and can help distinguish overlapping redox processes, it was used to further examine the concentration-dependent changes observed by CV.[14-16] In the absence of phosphine, $RuCl_3$ exhibited a prominent negative-potential feature near −0.73 V vs Ag wire. Addition of indoline shifted this feature to approximately −0.61 to −0.66 V and resulted in the appearance of additional electrochemical processes.

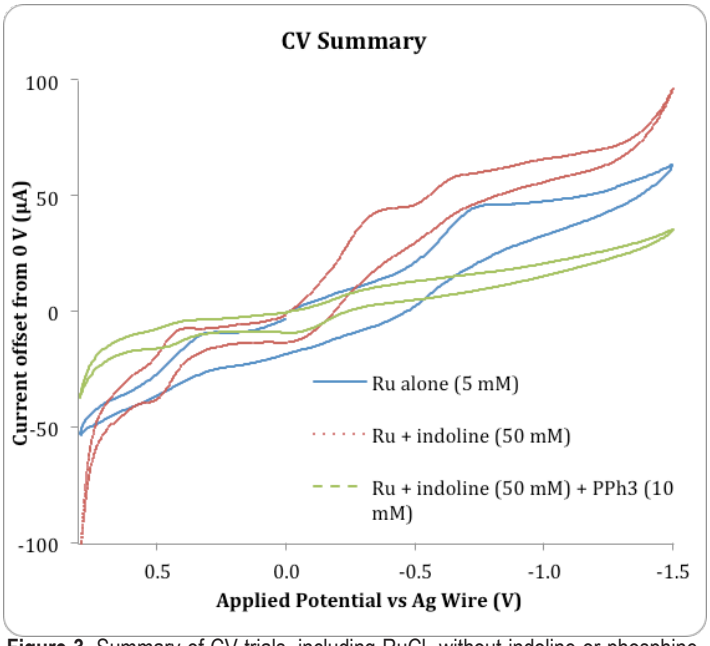


Figure 3. Summary of CV trials, including $RuCl_3$ without indoline or phosphine. For a more accurate visual comparison, each trace was vertically offset so that the current at 0 V applied potential was set to zero. No additional baseline correction was applied.

Most notably, at higher indoline concentrations a new positive-potential feature developed near +0.44 to +0.46 V. Thus, increasing indoline concentration does not simply increase the magnitude of the original $RuCl_3$ response, but instead generates a qualitatively different electrochemical profile, suggesting changes in ruthenium coordination, redox behavior, or both.

The presence of PPh_3 produced a distinctly different SWV response. Prior to addition of indoline, the $RuCl_3/PPh_3$ mixture displayed a major feature at approximately +0.396 V, together with features near +0.11, −0.18, and −0.66 V. Upon addition of indoline, the principal positive-potential feature shifted to approximately +0.428 V at 10 mM indoline and converged near +0.44 V at higher indoline concentrations, while another feature persisted near −0.15 to −0.18 V. Conversely, the feature near −0.65 V became progressively less prominent at higher indoline concentrations. These changes indicate that indoline affects multiple electrochemical responses in the phosphine-containing system, rather than producing a uniform increase or decrease in current. The substantially different responses observed in the presence and absence of PPh_3 are consistent with changes in ruthenium coordination and suggest competition among phosphine, indoline, acetonitrile, and potentially chloride for the coordination sphere of ruthenium. Considered with the CV results, the SWV data support the possibility that changes in ligand environment influence both the electrochemical behavior of ruthenium and subsequent chemical processes involving electrochemically generated species. However, the individual features cannot be assigned unambiguously to specific ruthenium oxidation states or intermediates based on these measurements alone.

Collectively, the CV and SWV experiments indicate that the electrochemical behavior of the ruthenium system is highly dependent on the ligand environment and do not support a simple, persistent Ru(III)/Ru(I) redox couple as the sole basis of the oxidation mechanism. Figure 3 provides a direct comparison of the electrochemical responses of $RuCl_3$ alone, $RuCl_3$ in the presence of indoline, and $RuCl_3$ in the presence of both indoline and PPh_3, highlighting the substantial changes that occur upon addition of these ligands. Instead, the data are more consistent with a dynamic mixture of ruthenium species undergoing coupled ligand-exchange, redox, and potentially subsequent chemical processes. Although the possibility that multinuclear ruthenium species or electronically coupled metal centers contribute to the observed electrochemical behavior cannot be excluded, the present data do not provide direct evidence for their formation. Thus, the observed voltammetric features are best interpreted as evidence of complex, ligand-dependent ruthenium redox chemistry rather than assigned to a specific multinuclear or mixed-valence structure.

Conclusion

In summary, we have explored the [Ru]-catalyzed oxidation of indoline derivatives to indoles using an in situ generated catalytic system under molecular oxygen. Optimization studies identified THF and controlled oxygen introduction as key parameters for efficient catalysis, affording up to 99% conversion and 94% isolated yield under the optimized conditions. Substrate scope investigations demonstrated that electron-rich indoline derivatives generally undergo oxidation more readily than electron-deficient substrates. Mechanistic studies involving phosphine ligands and cyclic voltammetry further revealed a strong sensitivity of the catalytic system to ligand sterics and electronics, while electrochemical experiments did not support the presence of a stable Ru(I) intermediate. Future studies employing spectroscopic techniques such as EPR will be valuable for further elucidating the nature of the active catalytic species and the mechanism of oxidation. These findings provide insight into the behavior of in situ generated Ru-based oxidation catalysts and may contribute to the future development of more efficient catalytic systems for indole synthesis.

Acknowledgments

We gratefully thank the L.S. & Aline Skaggs Research Fellowship and the Walter Maxwell Gibson Research Fellowship for the generous funding of this research.

References

1. Zeng, W.; Han, C.; Mohammed, S.; Li, S.; Song, Y.; Sun, F.; Du, Y. *RSC Med. Chem.* **2024**, *15* (3), 788–808.
2. Duan, S.-F.; Song, L.; Guo, H.-Y.; Deng, H.; Huang, X.; Shen, Q.-K.; Quan, Z.-S.; Yin, X.-M. *RSC Med. Chem.* **2023**, *14* (12), 2535–2563.
3. Fischer, E.; Jourdan, F. *Berichte Dtsch. Chem. Ges.* **1883**, *16*, 2241–2245.
4. Batcho, A. D.; Leimgruber, W. *Org. Synth.* **1985**, *63*, 214–220.
5. Bartoli, G.; Palmieri, G.; Bosco, M.; Dalpozzo, R. *Tetrahedron Lett.* **1989**, *30*, 2129–2132.
6. Larock, R. C.; Yum, E. K. *J. Am. Chem. Soc.* **1991**, *113* (17), 6689–6690. https://doi.org/10.1021/ja00017a059
7. Humphrey, G. R.; Kuethe, J. T. *Chem. Rev.* **2006**, *106*, 2875–2911.
8. Cacchi, S.; Fabrizi, G. *Chem. Rev.* **2005**, *105*, 2873–2920.
9. Keene, F. R.; Salmon, D. J.; Meyer, T. J. *J. Am. Chem. Soc.* **1976**, *98* (7), 1884–1889.
10. Keene, F. R. *Coord. Chem. Rev.* **1999**, *187* (1), 121–149.
11. Kuehne, M. E.; Hall, T. C. *J. Org. Chem.* **1976**, *41*, 2742–2746.
12. Diamond, S. E.; Tom, G. M.; Taube, H. *J. Am. Chem. Soc.* **1975**, *97* (10), 2661–2664.
13. Ray, R.; Hazari, A. S.; Lahiri, G. K.; Maiti, D. *Chem. – Asian J.* **2018**, *13* (17), 2138–2148.
14. Sandford, C.; Edwards, M. A.; Klunder, K. J.; Hickey, D. P.; Li, M.; Barman, K.; Sigman, M. S.; White, H. S.; Minteer, S. D. *Chem. Sci.* **2019**, *10*, 6404–6422.
15. Elgrishi, N.; Rountree, K. J.; McCarthy, B. D.; Rountree, E. S.; Eisenhart, T. T.; Dempsey, J. L. *J. Chem. Educ.* **2018**, 95, 197–206.
16. Rafiee, M.; Abrams, D. J.; Cardinale, L.; Goss, Z.; Romero-Arenas, A.; Stahl, S. S. *Chem. Soc. Rev.* **2024**, *53*, 566–585.
17. Morales-Rios, M. S.; Del Rio, R. E.; Joseph-Nathan, P. *Magn. Reson. Chem.* **1989**, *27*, 1039–1047.
18. Jiang, H.; Gao, S.; Xu, J.; Wu, X.; Lin, A.; Yao, H. *Adv. Synth. Catal.* **2016**, *358*, 188–194.
19. Yu, K.; Zhang, H.; Su, C.; Zhu, Y. *Eur. J. Org. Chem.* **2020**, *2020*, 1956–1960.